Preferred citation: X. Tong, W.H. Shen and X.-Q. Chen. Quantitative studies of ambient gases in pulp and paper mills and their degradation with photo-catalytic oxidation technology. In **Advances in Pulp and Paper Research, Oxford 2017**, *Trans. of the XVIth Fund. Res. Symp. Oxford, 2017*, (W. Batchelor and D. Söderberg, eds), pp 409–449, FRC, Manchester, 2018. DOI: 10.15376/frc.2017.1.409.

QUANTITATIVE STUDIES OF AMBIENT GASES IN PULP AND PAPER MILLS AND THEIR DEGRADATION WITH PHOTO-CATALYTIC OXIDATION TECHNOLOGY

Xin Tong, Wenhao Shen and Xiaoquan Chen*

State Key Laboratory of Pulp and Paper Engineering, South China University of Technology, Guangzhou, 510640, P.R. China

ABSTRACT

In order to reduce gaseous pollution emissions and achieve the goal of cleaner production in paper industry, in this study, (I) First, the concentrations of four potential compositions of gaseous pollutants, TVOC, HCHO, H_2S and C_xH_y, in the ambient air on 30 sampling sites in 5 pulp and paper mills were analysed. The analysed results were discussed in the following aspects: (a) the levels of four gaseous pollutants on all the sampling sites in five mills; (b) gaseous pollution differences due to different production processes; (c) gaseous pollution comparisons on the common sites. (II) Secondly, the compositions of VOCs in a secondary fiber paper mill were determined with GC-MS method. The main identified substances in the four sites were as follows: (a) waste paper sorting room: alkanes, phenols and esters; (b) paper machine hall: benzene homologues, alkanes, ethers and phenols; (c) vacuum pump outlet: benzene homologues and phenols; (d) office area: benzene homologues and phenols. (III) Third and last, aiming at the detected formaldehyde and benzene pollutants, a photo-catalytic reactor was developed and its performance with respect to degradation was studied. The performance tests of the reactor showed that both formaldehyde and benzene could be

completely degraded, but the degradation time for benzene was much longer than that for formaldehyde.

Key words: Gaseous pollutant, Paper mill, Analysis, Photo-catalytic, Degradation, GC-MS

1 INTRODUCTION

Being the sixth largest industry with respect to pollution in the world, pulp and paper mills not only emit large amounts of liquid and solid pollutants [1–4], but also discharge gaseous pollutants into the atmosphere, such as volatile organic compounds (VOCs), ozone, acetone, and formaldehyde [5,6]. In the gaseous pollutants discharged from paper mills, VOCs are the major gaseous emissions that not only cause environmental pollution, but also threaten human health [7,8]. Despite the possible environmental concerns and health risks, the analysis and degradation of gaseous pollutants in paper mills have not been the subject of public concerns for a long time, and there is not much research reported.

Concerning the treatment strategies of gaseous pollutants, the traditional methods include the condensation method [9], the absorption method [10], the adsorption method [11], the burning method [12], membrane separation technology [13], biological treatment technology [11], etc. Among these methods and technologies, photo-catalytic oxidation has attracted considerable attentions for degrading organics, given its advantages of powerful and non-selective oxidant active species [14,15]. A large number of VOCs with small and large molecular weights could be successfully photo-catalytically degraded under various conditions, indicating the excellent and non-selective ability of photo-catalytic oxidation technology to remove VOCs [16–18].

Aiming at the complementing the sparse studies on the gaseous pollutants in pulp and paper mills, this paper covers three parts, illustrated in Figure 1. (1) Firstly, the levels of TVOC, formaldehyde (HCHO), hydrogen sulfide (H_2S) and

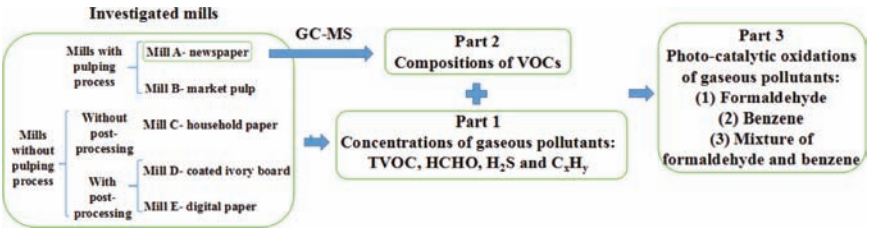

Figure 1. Roadmap of the research.

hydrocarbon (C_xH_y) in the air samples of five pulp and paper mills were quantified. (2) Secondly, further determination of the compositions of VOCs in the air samples were performed with GC-MS. (3) Finally, a novel treatment method of gaseous pollutants was introduced. By using nanoscale titanium dioxide particles as the core of the photo-catalysis oxidation technology, in combination with an intelligent control system, a photo-catalytic reactor was developed intended degrade two gaseous pollutants, formaldehyde and benzene.

2 CASE STUDIES

Five pulp and paper mills (Mills A-E) with different raw materials and final products were investigated, and their process schematics are presented in Figure 2. The information about the five mills were as follows: Mills A (offset newsprint) and B (market pulp board) are non-integrated, Mill C (household paper) is non-integrated and without converting, Mills D (coated ivory boards) and E (digital paper) are non-integrated but with converting. Six ambient air samples from different sites in each mill were collected and analysed (30 sites totally), whereof two sites were common to all five mills: the wet-end of paper machine and the wastewater treatment plant. Four compositions in each air sample were analysed: TVOC, HCHO, H_2S and C_xH_y.

Figure 2. Process schematics of five pulp and paper mills.

3 EXPERIMENTAL METHODS

3.1 Sampling and determination methods of ambient air samples in five mills

3.1.1 TVOC determination

By sampling each air sample for 15 minutes, the TVOC concentration was continuously measured in-situ by a portable gas detector, with a resolution of

1 ppb, having the air pump set at the flowrate of 220 mL·min^{-1} (FirstCheck+ 5000, Ion Science Ltd, UK). According to the instruction manual of FirstCheck, the detector measure the levels of TVOC by a PID (photo-ionisation detector) whose calibration and quantification were performed with isobutylene, and the data represented the levels of TVOC in the ambient air samples.

3.1.2 HCHO determination by UV/VIS spectrometer

The composition of HCHO in the air sample was collected with an air sampler (TWA-300Z, Tianyue Instrument Co., China) at a height of 1.5 meters from the ground, at a flowrate of 500 mL min^{-1} for 20 minutes, which meant that a total of 10 L of ambient air was collected each time. The collected air samples were immediately infiltrated by porous glass tubes where the distilled water was used as the absorption solutions for HCHO.

The Acetylacetone spectrophotometric method was adopted for the quantitative determinations of HCHO in the air samples [19,20]. In the presence of acetic acid-ammonium acetate and under boiling water condition of bath, the HCHO in the solution reacted with acetylacetone and generated yellow compounds, which were analysed by UV/VIS spectrometry (UV/VIS spectrophotometer S3001, Korea) at the wavelength of 413 nm. Based on the absorbance of the solution and the pre-determined calibration curve, the HCHO concentrations in the air samples were calculated with Eqs. (1) and (2):

$$c = \frac{(A\text{-}A_0\text{-}a) \times B_s}{V_0} \times \frac{V_1}{V_2} \tag{1}$$

$$V_0 = V_t \times \frac{T_0}{273+T} \times \frac{P}{P_0} \tag{2}$$

Where, V_0 – sampling volume under standard conditions, L;
V_t – sampling volume, L;
T – temperature at the sampling location, °C;
T_0 – absolute temperature under standard conditions, 273K;
P – atmospheric pressure at sampling time, kPa;
P_0 – atmospheric pressure under standard conditions, 101.3 kPa;
c – HCHO concentration in the ambient air, mgm^{-3};
A – absorbance of sample solution;
A_0 – absorbance of blank solution;
a – intercept of the calibration curve;
B_s – impact factor, μgabsorbance value^{-1};

V_1 – volume of absorbing solution, mL;
V_2 – sampling volume of absorbing solution, mL.

3.1.3 H_2S and C_xH_y determinations

The levels of H_2S and C_xH_y in the air samples were measured continuously on the sites by a Testo gas detector (350XL, Testo AG, Germany) for 15 minutes.

3.1.4 Standard-exceeding multiple of gaseous pollutants

The calculation method of the standard-exceeding multiple (SeM) of gaseous pollutants over the limits was given in Eq. (3).

$$\text{SeM} = \frac{\text{detected value-standard value}}{\text{standard value}} \tag{3}$$

The meanings of the signs of SeM value were as follows:

$$\begin{cases} = -1, \text{ meant no gaseous pollutants were detected;} \\ \in (-1, 0), \text{ meant the detected values of gaseous pollutants were below the limits;} \\ \geq 0, \text{ meant the detected values of the gaseous pollutants exceeded the standards.} \end{cases}$$

3.2 GC-MS analysis of VOCs in the ambient air samples

The air samples were collected by sampling with a glass tube containing activated carbon granules that were micro-porous materials (Tianyue Instrument Co., China). An air sampler (TWA-300Z, Tianyue Instrument Co., China) was used to pump air samples at a height of 1.5 meters and a flowrate of 500 mL min^{-1} for 20 minutes, which meant that a total of 10 L air was collected each time.

After sampling, the substances in the activated carbon tubes were extracted with two solvents, carbon disulfide (I) and dichloromethane (II). The detailed operations were as follows: (1) all the substances in the tubes were dissolved in 1 mL solvent by ultrasonication for 3 minutes; (2) the activated carbon granules were separated from the organic solvents by natural sedimentation for 30 minutes; (3) the supernatant solutions from Step two were obtained, which were named Sample I and Sample II.

The determination of the composition in Samples I and II was performed with a gas chromatograph coupled to a mass spectrometer (Varian-4000, Varian, Inc., USA). The DB-5MS capillary column of 60 m × 0.25 mm ID with 0.25 μm film thickness (Agilent J&W Scientific, USA) was used as the analytical column.

Table 1. GC-MS Parameters of Samples I and II

Parameters	*Sample I*	*Sample II*
Gas carrier	Helium	Helium
Gas flow	0.6 mL min^{-1}	1 mL min^{-1}
Injector	Splitless, 250 °C	Splitless, 250 °C
MS source temperature	200 °C	230 °C
Oven temperature	30 °C held 1 min; 10 °C min^{-1} to 60 °C; 30 °C min^{-1} to 150 °C, held 15 min.	40 °C for 2 min; 10 °C min^{-1} to 80 °C, held for 2 min; 25 °C min^{-1} to 260 °C, held 5 min.

Electron impact spectra were obtained with electron energy of 70 eV, and mass spectral data were acquired over a mass range of 33–350 amu. The detailed detection conditions of GC-MS for Samples I and II are presented in Table 1.

3.3 Photo-catalytic oxidation of gaseous pollutants

Combined with a microcontroller unit (MCU), our developed photo-catalytic reactor was mainly used for the degradation of VOCs detected in paper mills, which were represented by formaldehyde and benzene as the target pollutants.

3.3.1 Photo-catalytic reactor

An illustration of the photo-catalytic reactor can be found in Figure 3.

The reactor has three main components:

1) A filtering component for the removal of solid particles.
2) A photo-catalytic component to degrade the gaseous pollutants. It includes a maximum of three sets of honeycombs aluminium meshes coated with the titanium dioxide nanoparticles, which is subjected to the illumination of UV lamps.
3) A fan component to control the gas flowrate, which was used to adjust the residence time of the gas in the reactor.

In order to detect the concentrations of gaseous pollutants, a formaldehyde sensor (EC803-CH_2O, Bmoon), a portable benzene sensor (FirstCheck+ 5000, Ion Science Ltd, UK), and a digital temperature/humidity sensor (DHT11, Aosong) were mounted in the filter component. Finally, the gas flowrate could be controlled within 0–324 $m^3\ h^{-1}$ by the MCU. The photo-catalytic reactor has two operational modes; automatic and manual. Apart from allowing control of the MCU, a LCD

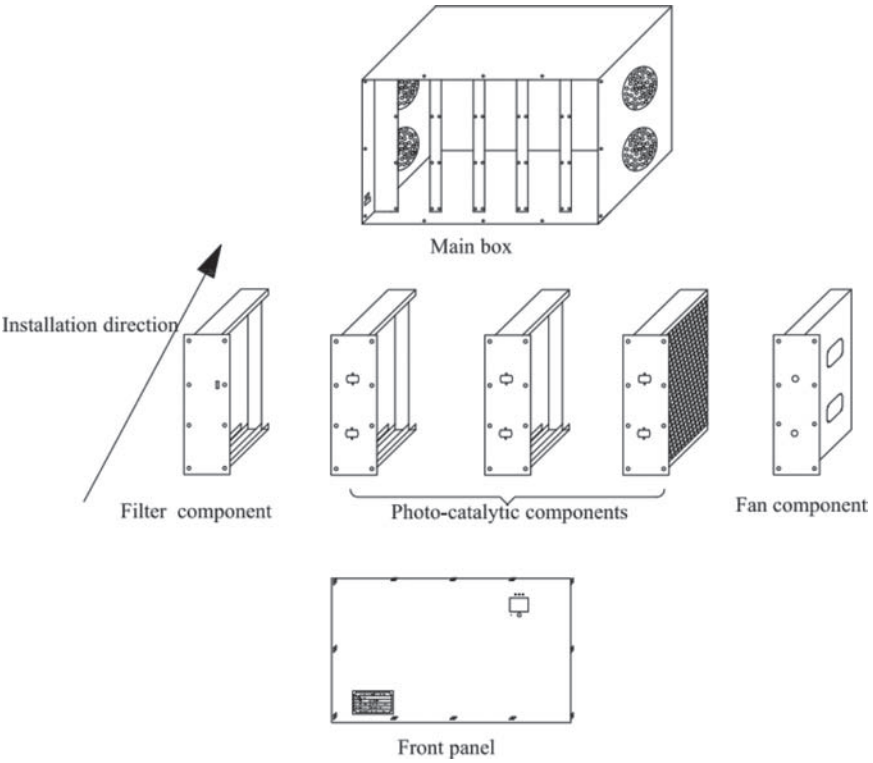

Figure 3. Schematic diagram of photo-catalytic reactor.

screen on the front panel of the reactor gives real-time indications of the concentrations of formaldehyde, benzene, temperature, humidity and fan speed during the photo-catalytic degradation of gaseous pollutants.

3.3.2 Degradation experiments

The degradation experiments of photo-catalytic reactor were conducted in the following sequence: blank experiments (Table 2), optimal experiments and degradation experiments. Among them, the formaldehyde was utilized as the target pollutants in the blank experiments and optimal experiments.

All the experiments were carried out in a closed cubic chamber (130 cm × 80 cm × 80 cm), which was used as the simulated gaseous environment of the paper mill. The data of gaseous pollutants, humidity and temperature in the

Table 2. Experimental conditions of blank experiments (√ means yes, × means no)

Ex. No.	*Experimental conditions*			*Objective*
	UV lamps	*Honeycomb aluminium nets*	*HCHO*	
1	√	×	√	Testing the effects of UV lamps on the degradation of formaldehyde.
2	√	×	×	Testing if the illumination of UV lamps cause pollution.
3	√	√	×	Testing the zero pollution from the photo-catalytic reactor.
4	×	√	×	Testing if the honeycomb aluminium nets themselves cause pollution.
5	×	×	×	Testing if the cubic chamber itself causes pollution.

chamber were quantitatively monitored by the above sensors mounted in the photo-catalytic reactor and were recorded every five minutes during all the experiments.

In the optimal experiments, three process elements were considered in the study: gas flowrates (32.4, 97.2, 162, 259.2 and 324 m^3h^{-1}), number of photo-catalytic components (1 set, 2 sets and 3 sets) and the size of the mesh (2 mm and 3 mm) of the honeycomb aluminium net.

The following reagents were utilized in the photo-catalytic experiments: formaldehyde solution (36%–38%) and pure liquid benzene (analytical reagent, 99.5%). The gaseous pollutants used in the photo-degradation study were obtained with the vapor from the above liquid solutions obtained through evaporated.

4 RESULTS & DISCUSSIONS

4.1 Analysis results of ambient air samples in five mills

4.1.1 Four compositions on all sampling sites

4.1.1.1 TVOC

The TVOC concentrations on all the sampling sites in five mills are presented in Figure 4, where the Chinese limit of 0.60 mg m^{-3} [21], is indicated by the dashed line and for the purpose of comparison, the averaged TVOC value of each mill is also listed on the tops of the columns.

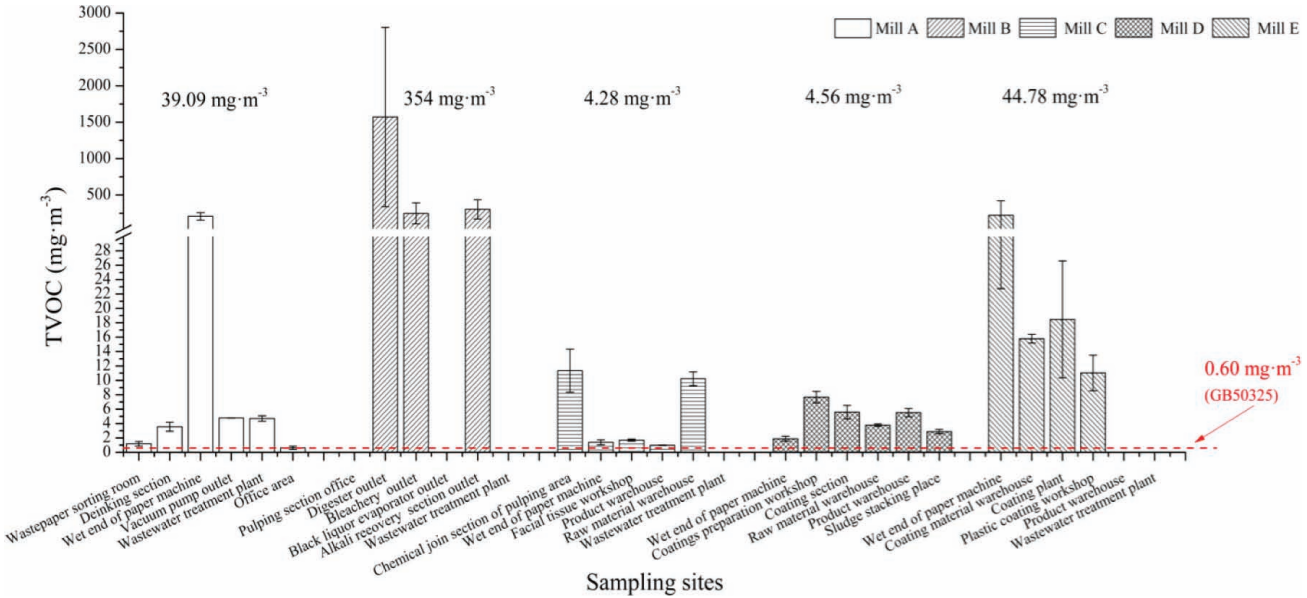

Figure 4. TVOC concentrations of the air samples on all the sampling sites in five mills (the dashed line is the Chinese limit for indoor pollution of TVOC in civil buildings).

Overall, the TVOC concentrations on 6 sites could not be detected, and the levels of the other 24 sites were above the limit. According to the TVOC average value of each mill, the ranking from high concentration to low was as follows: Mills B > E > A > D > C, wherein the TVOC average value of Mill B was extraordinary high, almost about 9 times higher than the second highest level.

Specifically, of the individual 30 sampling sites, two highest TVOC concentrations were all detected in Mill B, which were 1571.5 mg m^{-3} on the digester outlet and 304 mg m^{-3} on the alkali recovery section outlet, and their SeMs were 2618 times and 507 times, respectively. Following these were the wet-ends of paper machines in Mills A and E, and the bleachery outlet of Mill B, where the TVOC values were all around 200 mg m^{-3}, with SeMs close to 330. Moreover, the six zero-level sites covered three mills: wastewater treatment plant, one office area, one warehouse, and one black liquor evaporator outlet. Wherein notably, due to the height of the sampling point, the TVOC concentration of black liquor evaporator outlet in Mill B could not be detected, but it was necessary to indicate if there was any existence of TVOC.

The above data analysis indicated that the TVOC levels in Mill B and the wet-end of the paper machine of several mills were higher than others, the suggested reasons were as follows: In the pulping section, the pulping chemicals (anthraquinone, nonionic surfactants) and bleaching chemicals (H_2O_2, ethylene diamine tetraacetic acid), are the necessary additives for the pulping process; in the papermaking section, the process chemicals (retention and drainage aids), functional chemicals (polyvinyl alcohol, polyacrylic ester), pigments for fillers (synthetic dye, optical brightening agents), are often added to improve the properties of the products. All these chemical additives would have the capacity to be emission sources of VOCs in the pulping and papermaking process [22].

4.1.1.2 HCHO

The analysis results of HCHO on all the sampling sites are given in Figure 5, where the dashed line is the Chinese limit for indoor air quality of HCHO [23], and the average HCHO value of each mill is also given on the top of the columns for the purpose of comparison. As presented in Figure 5, except for the sludge stacking place in Mill D, the composition of HCHO were detected in 29 sites, wherein the HCHO levels on 22 sites exceeded the limit. Considering the average HCHO data of five mills, the SeM ranking from high to low were: Mills B (1.75) > C (1.30) > A (0.28) > E (0.03) > D (0).

Furthermore, as revealed in Figure 5, the alkali recovery section outlet and wastewater treatment plant in Mill B had the highest and second highest HCHO concentrations among all the sampling sites, which exceeded the limit by 4.54 and 2.91 times, respectively. The third highest site was detected on the wet-end of

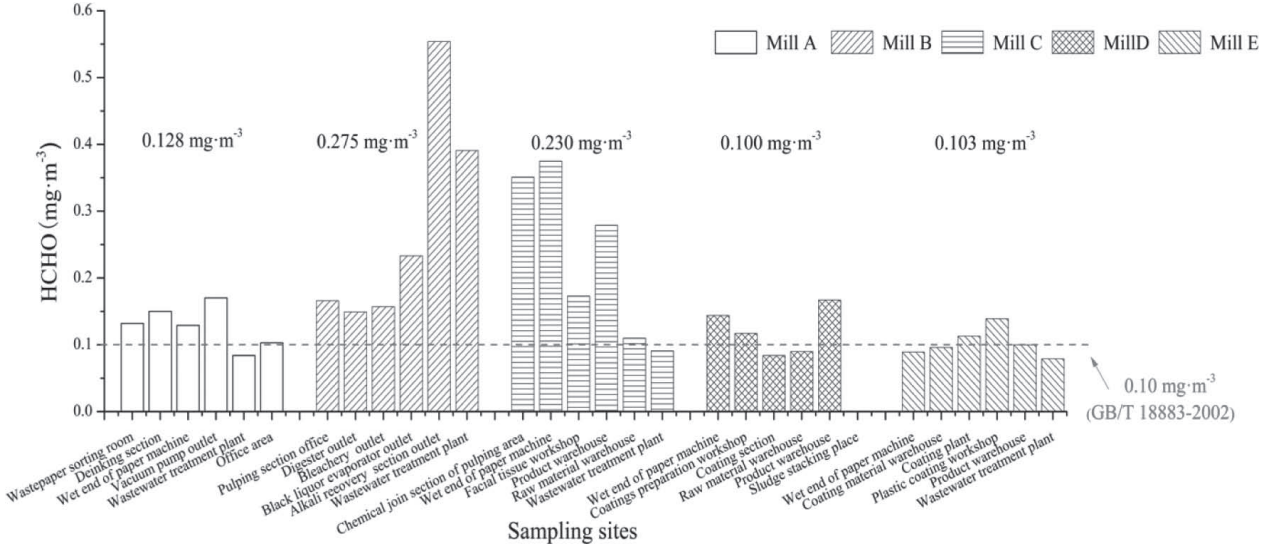

Figure 5. HCHO concentration of the air samples on all the sampling sites in five mills (the dash line is the Chinese standards for indoor air of HCHO).

paper machine of Mill C. In addition, the seven detection sites where the HCHO values were lower than the standard, covered three wastewater treatment plants, two warehouses, one coating section and one wet-end of paper machine.

4.1.1.3 H_2S

The concentrations of H_2S in the ambient air of 30 sampling sites are presented in Figure 6. According to the Chinese limits of malodorous gases, the emission standard of H_2S is 0.06 mg m^{-3}, which is shown as the dashed line in Figure 6 [24], and the average H_2S value is also listed on the top of the columns of each mill for the purpose of comparison.

Noticeably in Figure 6, despite of the great differences, all the detected H_2S data on the 30 sampling sites were in excess of the limit significantly. Wherein, the three highest concentrations of H_2S were all found in Mill B, which exceeded the limit by 1640, 1455, and 962 times, respectively. Consequently, the average value of H_2S in Mill B was the highest one among five mills, which was even higher than any sites in other four mills. From high to low, the average H_2S value of each mill was as follows: Mills B > A > D > E > C.

4.1.1.4 C_xH_y

The corresponding threshold limit values of hydrocarbons (C_1–C_8) were specified as 385–1000 ppm by NIOSH (National Institute for Occupational Safety and Health) [25, 26], which are plotted as two dashed lines in Figure 7, and the average C_xH_y value of each mill is also listed on the top of each column for the purpose of comparison. As displayed in Figure 7, the ranking of the average C_xH_y value was as follows: Mills B > A > C > D > E. The highest average concentration found in the five mills was 1952 ppm in Mill B. Although the office area in Mill A (6930 ppm) had the highest concentration among all the 30 sampling sites, the lowest was also located in the same mill at the vacuum pump outlet (10 ppm). Totally, the average C_xH_y concentration in Mill A was 1470 ppm, which ranked second behind Mill B of the five mills.

Setting 1000 ppm as the discharge limit of C_xH_y, the highest level of 6930 ppm in the office area of Mill A exceeded the limit 5.93 times. In addition to the above site, the C_xH_y concentrations on the other five sites also exceeded the limit, whereof four in Mill B.

Summing up the above detected results, the highest SeMs of four pollutants were all revealed in Mill B, which can be seen in Table 3. The above facts showed that the situation of gaseous pollution in the integrated mill was much more serious than those in non-integrated mills.

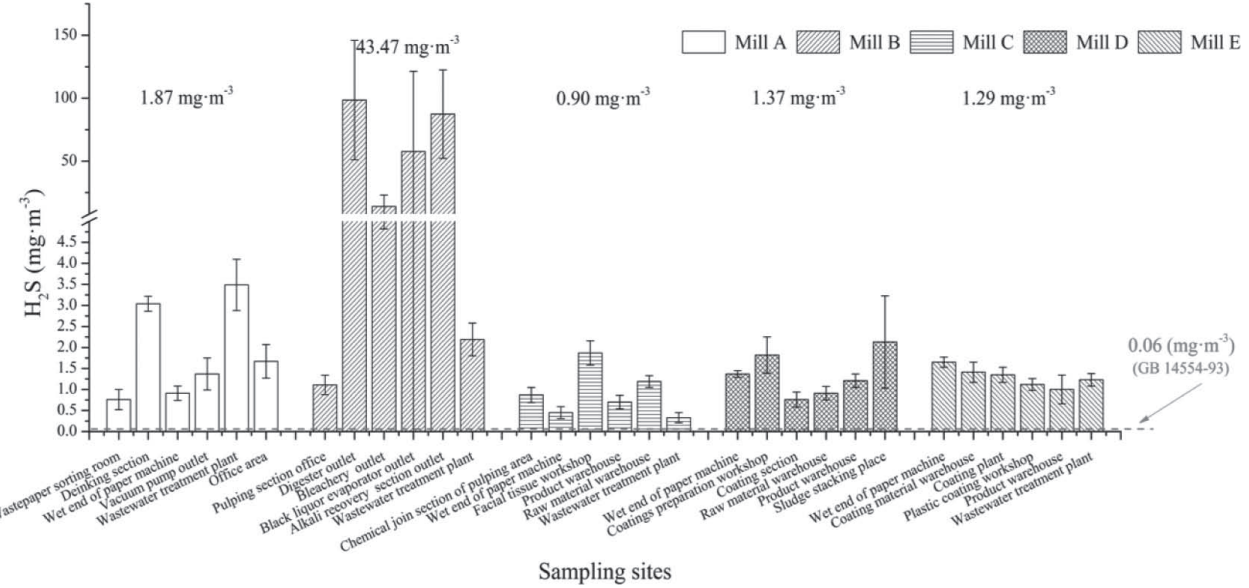

Figure 6. H_2S concentration of the air samples on all the sampling sites in five mills (the dash line is the Chinese emission standard for H_2S).

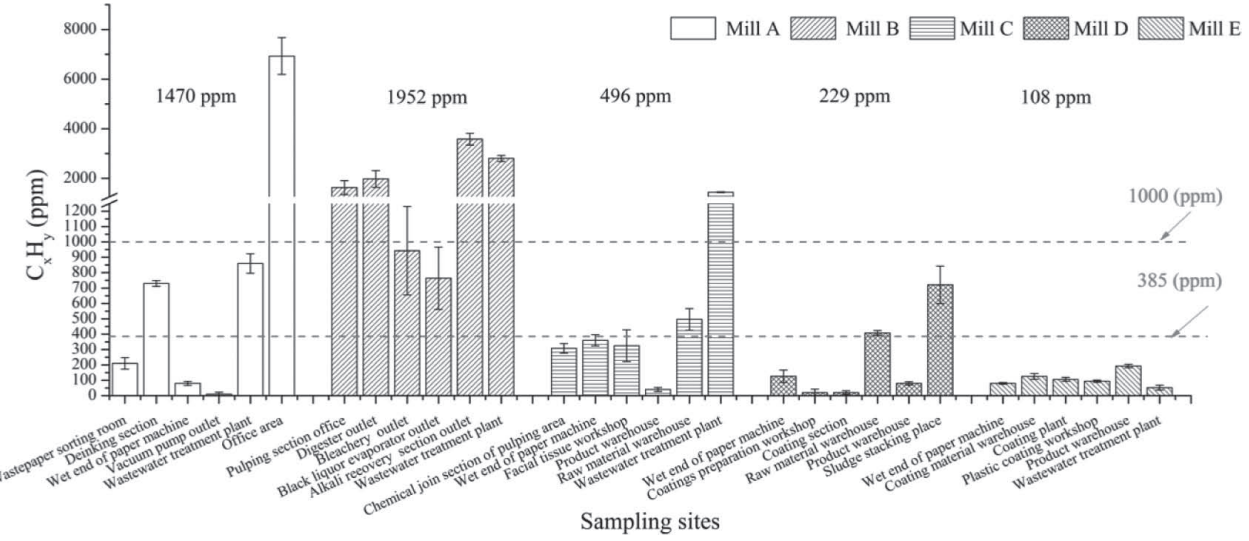

Figure 7. C_xH_y concentrations of the air samples on all the sampling sites in five mills (The dash lines are the NIOSH quality standards for the indoors C_xH_y (C_1–C_8) specified as 385–1000 ppm).

Table 3. Average SeMs of four compositions in five mills

Composition	*Mills with pulping process*		*Mills without pulping process*		
			Mill without post-processing	*Mills with post-processing*	
	Mill A	*Mill B*	*Mill C*	*Mill D*	*Mill E*
TVOC	60.83	589.50	6.35	6.59	73.46
HCHO	0.28	1.75	1.30	0.00	0.03
H_2S	30.22	723.53	14.03	21.78	20.57
C_xH_y	0.47	0.95	–0.50	–0.77	–0.89

4.1.2 Production process distinctions

After evaluating the overall gaseous pollution from all the 30 sampling sites in five mills, the pollution situations in each mill were studied in detail. According to the production process distinctions, as listed in Figure 1, the five mills were classified into two groups: mills with/without pulping process, and the detailed results are presented in the following.

4.1.2.1 Mills with pulping process (Mills A and B)

The overall analysis results of TVOC, HCHO, H_2S and C_xH_y substances in the air samples of Mills A and B are shown in Figures 8 and 9 individually. The SeMs of TVOC, HCHO, H_2S, and C_xH_y (calculated by the high limit 1000 ppm) are indicated on the top of each column, and are also listed in Tables 4 and 5, respectively.

As revealed in Tables 4 and 5, TVOC and H_2S were the major gaseous pollutants in Mills A and B, and the SeMs of Mill B were much higher than those of Mill A. In particular, as presented in Figure 8, the four gaseous pollutants in the ambient air samples on the digester outlet and the alkali recovery section outlet in Mill B exceeded the limits significantly, especially the TVOC level from the former location. The H_2S levels from both of these two sites exceeded the limits by 2618, 1640, and 1455 times, respectively.

These detected results suggested that, although both of Mills A and B includes the pulping process, when compared with the secondary fibre pulping in Mill A, the gaseous pollutions in Mill B (virgin fibre) were much more serious. When comparing Mill A with Mill B, the pulping process of Mill B was more complicated. In the

pulping process of Mill B, the wood chips are cooked with the steam and the alkaline cooking liquor, which contains NaOH, NaS_2, Na_2CO_3, Na_2SO_4, Na_2SO_3, and $Na_2S_2O_3$. The kraft process is a process where the lignin in the wood degrading into the spent liquor [27,28]. Furthermore, in order to recycle the inorganic compounds of Na_2CO_3 and Na_2S, the subsequent processes of evaporation and alkali recovery after pulping are performed to concentrate and burn the spent liquid from the bleaching process. These processes are actually a methane synthesis unit where the small organic molecules, such as carboxylic acid, alcohols and aldehydes, are converted to CH_4, C_2H_x, CO_2, H_2, and CO [29]. Hence, that was the reason why the compositions of HCHO and C_xH_y in the ambient air sample from alkali recovery section outlet were the highest ones among the six sampling sites in Mill B (Figure 10), and their SeMs were 4.54 times and 2.59 times, respectively.

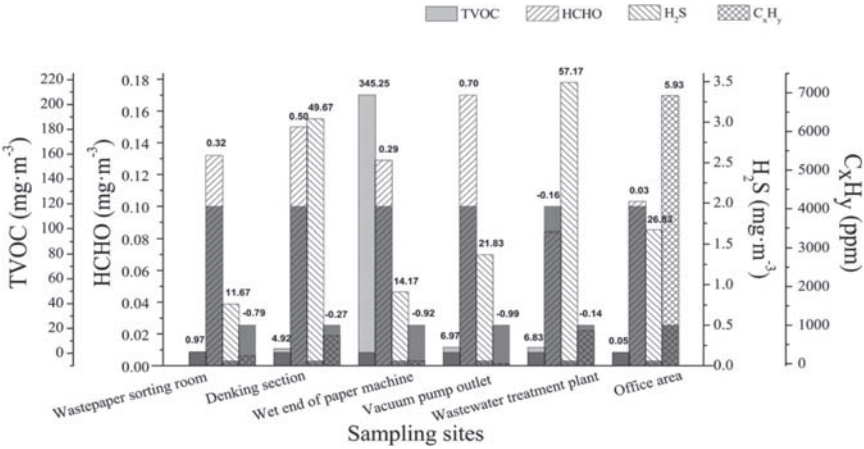

Figure 8. Four composition levels in the air samples of Mill A (the columns in dark grey colour are the standards for the corresponding pollutants).

Table 4. SeMs of four pollutants in Mill A

Sampling site	*TVOC*	*HCHO*	*H_2S*	*C_xH_y*
Wastepaper sorting room	0.97	0.32	11.67	–0.79
Deinking section	4.92	0.50	49.67	–0.27
Wet-end of paper machine	345.25	0.29	14.17	–0.92
Vacuum pump outlet	6.97	0.70	21.83	–0.99
Wastewater treatment plant	6.83	–0.16	57.17	–0.14
Office area	0.05	0.03	26.83	5.93

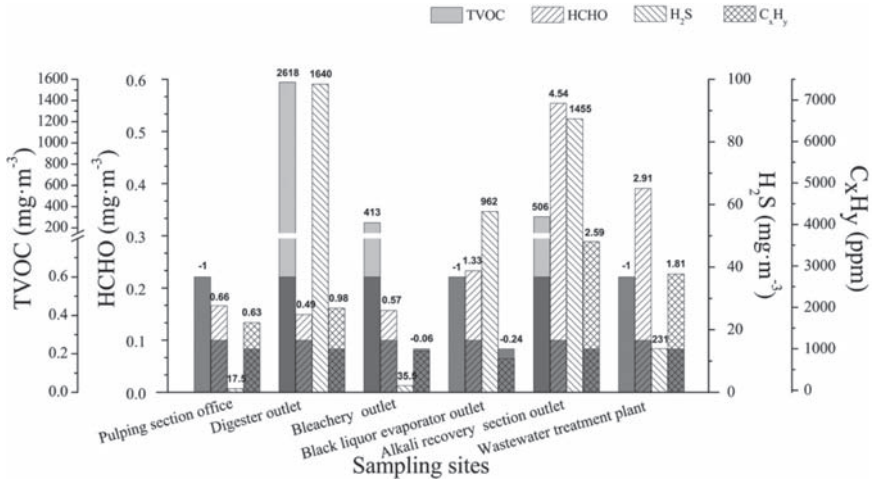

Figure 9. Four composition levels in the air samples of Mill B (the columns in dark grey colour are the standards for the corresponding pollutants).

Table 5. SeMs of four compositions in Mill B

Sampling site	*TVOC*	*HCHO*	*H_2S*	*C_xH_y*
Pulping section office	–1	0.66	17.50	0.63
Digester outlet	2618	0.49	1640	0.98
Bleachery outlet	413	0.57	35.50	–0.06
Black liquor evaporator outlet	–1	1.33	962	–0.24
Alkali recovery section outlet	506	4.54	1455	2.59
Wastewater treatment plant	–1	2.91	231	1.81

4.1.2.2 Mills without pulping process (Mills C, D and E)

Although all the raw materials for Mills C, D and E were commercial pulp board, which meant that they had no pulping process, these three mills were also different and classified into two groups: with/without converting. Their four gaseous pollutants were discussed as the following order: Mills D, E and C.

As presented in Figure 10 and Table 6, although the TVOC on the six sites in Mill D exceeded the limits, the highest level of TVOC was detected on the site of the coater and exceeded the limit by 11.79 times. As displayed in Figure 11 and Table 7 of Mill E, except for the sampling sites at the product warehouse and the wastewater treatment plant, the presence of TVOC in Mill E, all above the limit, were revealed. Moreover, another pollutant in Mills D and E was H_2S, as displayed

in Table 3, although the differences between the average SeMs in two mills were minor, the H_2S content on the wastewater treatment plant in Mill D (Figure 10, Table 6) exceeded the limit 34.5 times, which was higher than that (19.5 times) in Mill E (Figure 11, Table 7).

The product of Mill E was plastic coated digital paper having a strong water-resistance. In producing the baese-layer for the plastic coated paper, many kinds of additives were used in the papermaking process, such as acrylic acid, acrylamide, polyethylene, and sodium stearate. These chemical additives resulted in the highest contents of TVOC and H_2S on the wet-end of paper machine in Mill E, exceeding the limits 368 and 26.5 times, respectively (Figure 11).

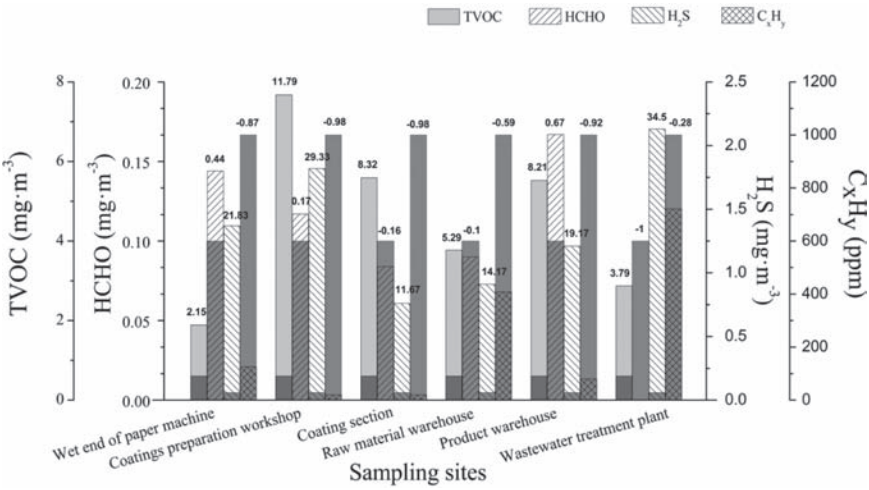

Figure 10. Four composition levels in the air samples of Mill D (the columns in dark grey colour are the standards for the corresponding pollutants).

Table 6. SeMs of four compositions in Mill D

Sampling site	*TVOC*	*HCHO*	*H_2S*	*C_xH_y*
Wet-end of paper machine	2.15	0.44	21.83	–0.87
Coating preparation workshop	11.79	0.17	29.33	–0.98
Coating section	8.32	–0.16	11.67	–0.98
Raw material warehouse	5.29	–0.10	14.17	–0.59
Product warehouse	8.21	0.67	19.17	–0.92
Wastewater treatment plant	3.79	–1	34.50	–0.28

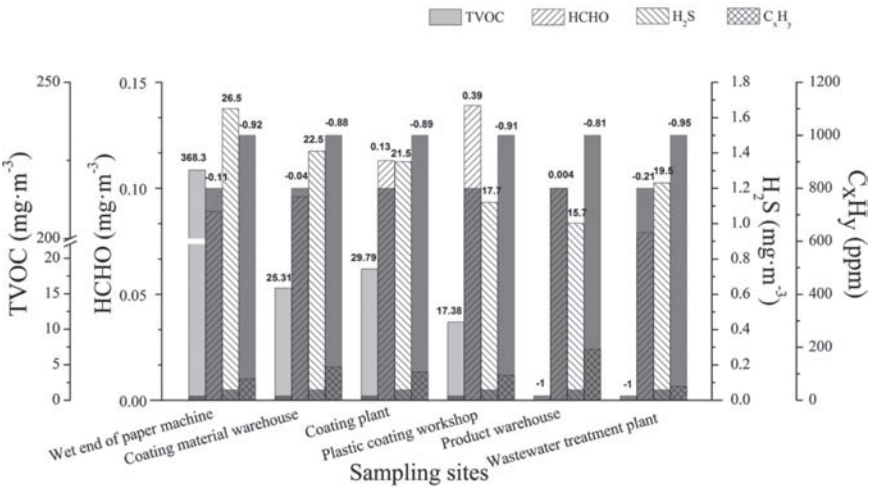

Figure 11. Four composition levels in the air samples of Mill E (the columns in dark grey colour are the standards for the corresponding pollutants).

Table 7. SeMs of four compositions in Mill E

Sampling site	*TVOC*	*HCHO*	*H_2S*	*C_xH_y*
Wet-end of paper machine	368.30	–0.11	26.50	–0.92
Coating material warehouse	25.31	–0.04	22.50	–0.88
Coating plant	29.79	0.13	21.50	–0.89
Plastic coating workshop	17.38	0.39	17.67	–0.91
Product warehouse	–1	0.004	15.70	–0.81
Wastewater treatment plant	–1	–0.21	19.50	–0.95

Except for the sludge stacking place, the presence of HCHO was detected at all other sampling points in Mill D. As displayed in Figure 10, due to the large amount of coated paperboard stored in the product warehouse, the HCHO content in the ambient air in the product warehouse in Mill D was the highest one. Unlike Mill D, as disclosed in Figure 11, the highest level of HCHO in Mill E was not detected on the product warehouse, but in the coating workshop where the chemical additives, like polyethylene, gelatine and emulsion, were applied. This result demonstrates that the chemical agents used in the coating process were the emission sources of HCHO in Mill E.

With respect to the details of gaseous pollution in Mill C, as plotted in Figure 12 and Table 8, the contents of TVOC in the air samples from the chemical dosage section of the pulp shredder and the raw material warehouse exceeded the

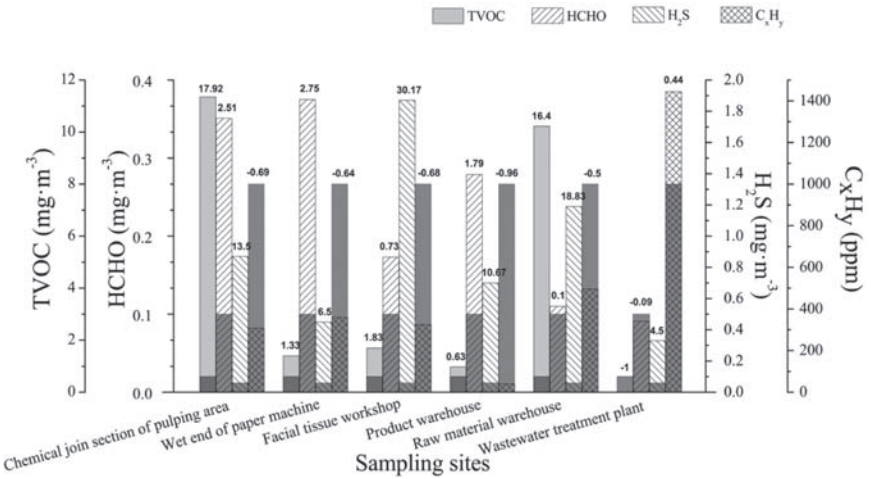

Figure 12. Four composition levels in the air samples of Mill C (the columns in dark grey colour are the standards for the corresponding pollutants).

Table 8. SeMs of four compositions in Mill C

Sampling site	*TVOC*	*HCHO*	*H_2S*	*C_xH_y*
Chemical join section of pulp shredder	17.92	2.51	13.50	–0.69
Wet-end of paper machine	1.33	2.75	6.50	–0.64
Facial tissue workshop	1.83	0.73	30.17	–0.68
Product warehouse	0.63	1.79	10.67	–0.96
Raw material warehouse	16.40	0.10	18.83	–0.50
Wastewater treatment plant	–1	–0.09	4.50	0.44

limit by 17.92 and 16.4 times respectively; HCHO was found mainly at the wet-end of paper machine and the chemical dosage section of the pulp shredder; although the average SeM of H_2S in Mill C was the lowest one in five mills (Table 3), the H_2S level in the ambient air of the facial tissue workspace was still high due to the application of the sulphur-containing flavour. Specifically, the mercaptan fragrance compounds are important sulphur spices that contribute to the flavours with tropical fruit and plant, which was the main types of aroma in the products of Mill C [30, 31]. C_xH_y was only detected in the wastewater treatment plant, which exceeded the limit by 1.44. These data obtained in Mill C can be explained as follows: using market pulp board as the raw material, it's chemical additives, such as fillers, softeners and dispersion agents, becomes the main sources of TVOC and HCHO in Mill C.

The above detected levels in mills without a pulping process suggests that: the different requirements of the final products for each mill results in the applications of multiple flavours (Mill C), coating laminate materials (Mills D and E) and additives (Mills C, D and E) in their production processes, and finally influenced the gaseous pollutants distributions in these mills.

4.1.3 Results comparisons on the common sites

In order to understand more about the influence of production technologies on the gaseous pollution, the comparisons of the gaseous pollutions on two similar sites at these five mills were made: (I) the wet-end of the paper machines, and (II) the wastewater treatment plant.

Except for Mill B (a pulp mill), Mills A, C, D and E have papermaking operations in which the wet-end of paper machines are present. In general, about 90% of the paper chemicals used to improve the paper properties are added in the wet-end. Moreover, due to the consumption of large quantities of water, the wastewater treatment plant is always an integral part for the paper industry. Hence, the gaseous pollutions in the wastewater treatment plant in each mill were particularly concerned in the study.

The detected values of four kinds of gaseous pollutants on these two common sites are presented in Figures 13, 14 and Table 9.

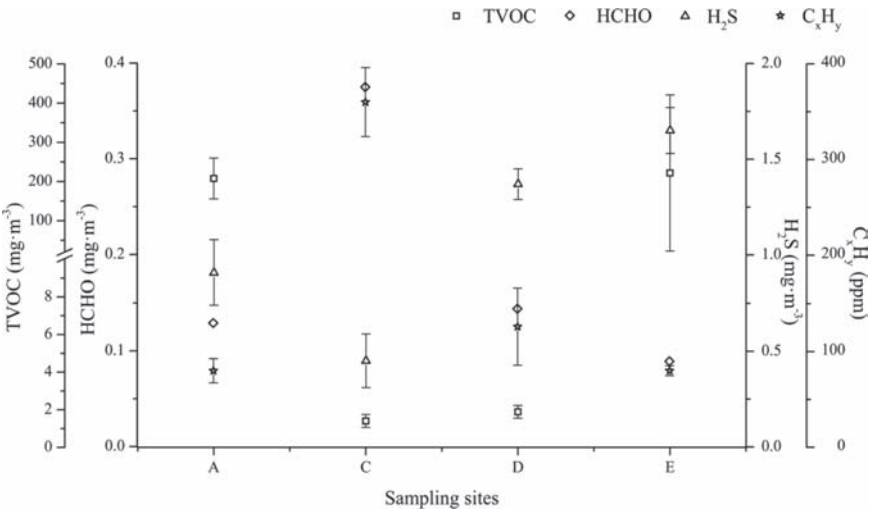

Figure 13. Four composition levels in the air samples of the wet-end of paper machines in Mills A, C, D and E.

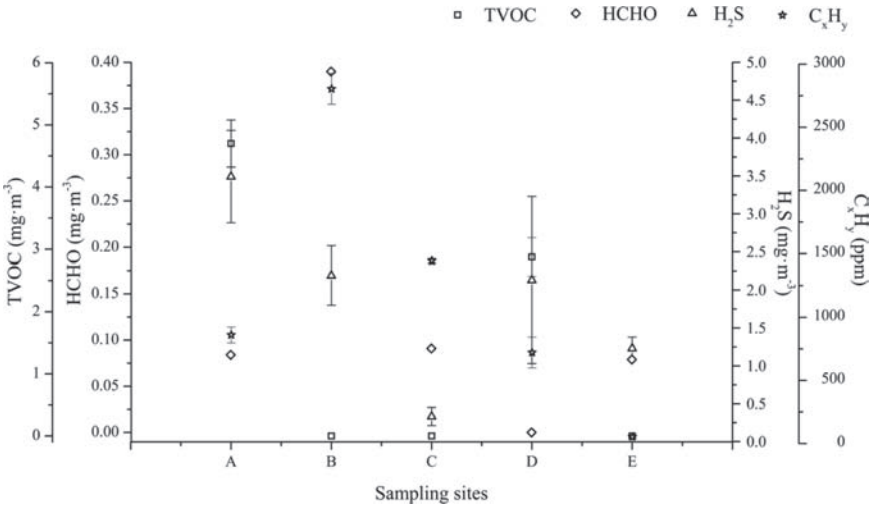

Figure 14. Four composition levels in the air samples of the wastewater treatment plants in Mills A, B, C, D and E.

Table 9. SeMs of four compositions in the air samples of two common sites in five mills

Composition	(I) Wet-end of paper machine				(II) Wastewater treatment plant				
	A	C	D	E	A	B	C	D	E
TVOC	345.25	1.33	2.15	368.30	6.38	–1	–1	3.79	–1
HCHO	0.29	2.75	0.44	–0.11	–0.16	2.91	–0.09	–1	–0.21
H_2S	14.17	6.50	21.83	26.50	57.15	231	4.50	34.50	19.50
C_xH_y	–0.92	–0.64	–0.87	–0.92	–0.14	1.81	0.44	–0.28	–0.95

From the data in Table 9, the rating of the average SeMs of four compositions on two common sites were obtained as follows:

- Wet-end of paper machine:
  - TVOC (179.26) > H_2S (17.25) > HCHO (0.84) > C_xH_y (–0.84).
- Wastewater treatment plant:
  - H_2S (69.33) > TVOC (1.43) > HCHO (0.29) > C_xH_y (0.18).

A comparison of these results shows that, although both of the most two serious gaseous pollutants on the two common sites were TVOC and H_2S, their levels (above the limits) were very different. In absolute terms, TVOC and H_2S were the most two serious gaseous pollutants in the wet-end of paper machine and the

wastewater treatment plant, respectively. These two main pollutants could be attributed to the following: (1) The application of huge quantities of paper chemicals (dyes, coating binders, reinforced strength and sizing agents, etc.) in the wet-end of paper machine. (2) In the wastewater treatment plant, with the effects of sulphate-reducing bacteria, the sulphate in the wastewater was reduced to H_2S through microbial action under anaerobic conditions.

Summing up the results on gaseous pollutants in five pulp and paper mills in Section 4.1, the following points could be summarized: the levels of TVOC, HCHO, H_2S, and C_xH_y in the pulp mills were much higher than those in paper mills; different raw materials and applied paper chemicals could largely influence the gaseous pollutions in paper mills.

4.2 GC-MS analysis results of VOCs in the ambient air samples

The results in Section 4.1 show that TVOC is one of the main gaseous pollutants in paper mills. In order to study the detailed composition of TVOC, sampling of the ambient air was further pursued on four sites in Mill A (pulping with secondary fibre and papermaking). As described in Section 3.2, desorbing with carbon disulfide and dichloromethane individually, the compositions of VOCs in the air samples were determined.

4.2.1 Site A-waste paper sorting area

In this area, with the extraction of carbon disulfide, the analysed results of Sample I in Table 10 revealed that all the detected substances were alkane compounds with high boiling point. It was surmised that during the collection and transportation process of waste paper, some compounds with high boiling points might attach to the dust and particulate matter on the surface of the waste paper, thus they were adsorbed on the activated carbon during the sampling process.

With the extraction of the weak polar solvent (dichloromethane), the information in Table 10 showed that the following substances were detected in the waste paper sorting room and their relative quantities were: phenols (57%), esters (38%), alkanes (3%) and ketones (2%) [32].

The above analysed results of the desorption with two solvents revealed that: there were mainly alkane compounds, phenols, and esters with high boiling points in the waste paper sorting room of this secondary fiber paper mill.

4.2.2 Site B-wet-end of paper machine

The mass spectra of the air samples from the papermaking workshop with two extraction solvents are shown in Table 11. It shows that by extraction using

Table 10. GC-MS analytical results of air sample from waste paper sorting room in Mill A

Carbon disulfide (Sample I)				*Dichloromethane (Sample II)*			
No.	*Organic pollutant*	*Molecular formula*	*Matching degree (%)*	*No.*	*Organic pollutant*	*Molecular formula*	*Matching degree (%)*
1	Nonadecane	$C_{19}H_{40}$	95	1	2-Hydroxy-1-phenylethanone	$C_8H_8O_2$	95
2	n-Heneicosane	$C_{21}H_{44}$	75	2	cis-9-Heneicosene	$C_{21}H_{42}$	77
3	Tetracosane	$C_{24}H_{50}$	90	3	Methyl hexadecanoate	$C_{17}H_{34}O_2$	62
4	Octacosane	$C_{28}H_{58}$	85	4	13-Methyl Pentadecanoic acid methyl ester	$C_{17}H_{34}O_2$	60
				5	2,2′-Methylenebis (6-tert-butyl-4-methylphenol)	$C_{23}H_{32}O_2$	71

Table 11. GC-MS analytical results of air sample from papermaking workshop in Mill A

Carbon disulfide (Sample I)				*Dichloromethane (Sample II)*			
No.	*Organic pollutant*	*Molecular formula*	*Matching degree (%)*	*No.*	*Organic pollutant*	*Molecular formula*	*Matching degree (%)*
1	Carbon disulfide	CS_2	97	1	2-Hydroxy-1-phenylet hanone	$C_8H_8O_2$	95
2	Benzene	C_6H_6	94	2	Butylated hydroxyl-anisole	$C_{11}H_{16}O_2$	71
3	Methyl-benzene	C_7H_8	93	3	Heptadecane	$C_{17}H_{36}$	82
4	p-xylene	C_8H_{10}	88	4	2,4,5-triisopropyl-phenol	$C_{15}H_{24}O$	65
5	Ethylbenzene	C_8H_{10}	70	5	9-Acridone	$C_{13}H_9NO$	81
6	2-Ethyltoluene	C_9H_{12}	90	6	Ditolyl-methane	$C_{15}H_{16}$	77
7	Decane	$C_{10}H_{22}$	41	7	Methyl pentadecan-oate	$C_{16}H_{32}O_2$	66
8	Dodecane	$C_{12}H_{26}$	39				

carbon disulfide as solvent, Sample I contains benzene, methylbenzene, p-xylene, ethylbenzene, 2-ethyltoluene, decane and dodecane, etc., while Sample II and extraction with dichloromethane solvent contains ketones (5%), ethers (12%), alkane compounds (64%), esters (6%), and phenols (13%).

The results above demonstrate that some hazardous substances, including the benzene homologues, alkane compounds, phenols, ethers, etc., were present in the papermaking workshop, where many chemical additives often are added.

4.2.3 Site C-vacuum pump outlet

Ambient gas in the papermaking workshop is often collected by an exhaust hood and discharged into the atmosphere using vacuum pumps. The mass spectra obtained by GC-MS analysis are listed in Table 12.

It can be clearly seen that in Sample I, more benzene homologues (1,3-dimethyl benzene, 2,5-dimethyl-2-amino propyl benzene, 1-allyl mercaptan, heptane) could be detected in the vacuum pump outlet. Being different from the results of Sample I, in Table 12, Sample II and the extraction with dichloromethane as solvent in this location showed different compositions, including phenols, esters, ketones and olefins. This result could be attributed to the high temperature in the vacuum pump outlet, VOCs in the hot ambient air are more likely to volatilize and be adsorbed by the activated carbon.

In short, although there were more substances detected in the vacuum pump outlet than on other sites, the main compositions were made up of benzene homologues and phenols in large quantities.

4.2.4 Site D-office area (near the wastewater treatment plant)

All the interpretations of the mass spectra of two samples in the office area are listed in Table 13. It could be observed that: the GC-MS results of Sample I contained only two substances, benzene and methylbenzene; while several compounds were detected in Sample II, and phenols (93%) were the main substance.

Compared to the detected results on the other three sites in Mill A, it should be noted that the composition of VOCs in the office area was relatively different, only two main substances were detected: benzene homologues and phenols. Although the office area was one kilometre away from the production area, the hazardous substances in the ambient air of the production area could also diffuse to the office area.

Before ending Section 4.2, the following points can be concluded: Two main toxic substances in VOCs, benzene homologues and phenols, were detected in the ambient air of the Mill A. And therein the benzene homologues existed in the three detected sites in the main process of papermaking, and even in the office

Table 12. GC-MS analytical results of air sample from vacuum pump outlet in Mill A

Carbon disulfide (Sample I)				*Dichloromethane (Sample II)*			
No.	*Organic pollutant*	*Molecular formula*	*Matching degree (%)*	*No.*	*Organic pollutant*	*Molecular formula*	*Matching degree (%)*
1	Carbon disulfide	CS_2	98	1	2,2-Dimethylpropiophenone	$C_{11}H_{14}O$	79
2	Benzene	C_6H_6	95	2	Methyl nonadecanoate	$C_{20}H_{40}O_2$	55
3	Methyl-benzene	C_7H_8	93	3	cis-9-Heneicosene	$C_{21}H_{42}$	79
4	p-xylene	C_8H_{10}	80	4	cis-11-Tetradecenyl acetate	$C_{16}H_{30}O_2$	77
5	Ethylbenzene	C_8H_{10}	63	5	Methyl 2-methyltetradecanoate	$C_{16}H_{32}O_2$	67
6	o-xylene	C_8H_{10}	50	6	2,2′-Methylenebis(6-tert-butyl-4-methylphenol)	$C_{23}H_{32}O_2$	70
7	1, 3 – Dimethyl benzene	C_8H_{10}	52				
8	2-Ethyltoluene	C_9H_{12}	70				
9	Cumene	C_9H_{12}	83				
10	1, 2, 3 – Trimethyl benzene	C_9H_{12}	40				
11	2, 5 – Dimethyl – 2 – amino propyl benzene	$C_{11}H_{17}N$	60				
12	Allyl mercaptan	C_3H_6S	35				
13	Heptane	C_7H_{16}	56				

Table 13. GC-MS analytical results of air sample from office area in Mill A

Carbon disulfide (Sample I)				*Dichloromethane (Sample II)*			
No.	*Organic pollutant*	*Molecular formula*	*Matching degree (%)*	*No.*	*Organic pollutant*	*Molecular formula*	*Matching degree (%)*
1	Carbon disulfide	CS_2	97	1	2-Hydroxy-1-phenylethanone	$C_8H_8O_2$	96
2	benzene	C_6H_6	86	2	cis-9-Heneicosene	$C_{21}H_{42}$	82
3	methylbenzene	C_7H_8	90	3	2,4,6-Trimethyldecane	$C_{13}H_{28}$	88
				4	7-Methylpentadecane	$C_{16}H_{34}$	78
				5	Methyl hexadecanoate	$C_{17}H_{34}O_2$	61
				6	2,2′-Methylenebis(6-tert-butyl-4-methylphenol)	$C_{23}H_{32}O_2$	72

area, which was far away from the production line. Additionally, phenols were detected on all the sampling locations.

4.3 Photo-catalytic oxidation of gaseous pollutants in paper mills

The detected results in Section 4.1 and the analysis results with GC-MS in Section 4.2 showed that TVOC and benzene homologues were the main gaseous pollutants in pulp and paper mills. Aiming at these results, a photo-catalytic reactor was developed to degrade these detected main gaseous pollutants, which were applied with formaldehyde and benzene as the target pollutants.

Playing an important role in the photo-catalytic reactor, as illustrated in Figure 3, the photo-catalytic component was composed of three sets of aluminium meshes with coated with titanium dioxide nanoparticles. Prior to the photo-catalytic degrading experiments, a honeycomb aluminium mesh was studied. Its morphology was characterized (scanning electron microscopy (SEM)) in the direction perpendicular to the gas flow (Figure 14(a)), and the surface element distribution study (energy dispersive spectrometer (EDS)) in the direction parallel, (Figure 15(b)) to the gas flow, demonstrated that the surface of the net was covered with the spherical titanium dioxide nanoparticles with an average size of 15 nm (Figure 15(a)), and the surface of the mesh contained the elements of oxygen, aluminium and titanium (Figure 15(b)). These characterization results show that the titanium dioxide nanoparticles give a huge specific surface area, which was is beneficial to the degradation of gaseous pollutants.

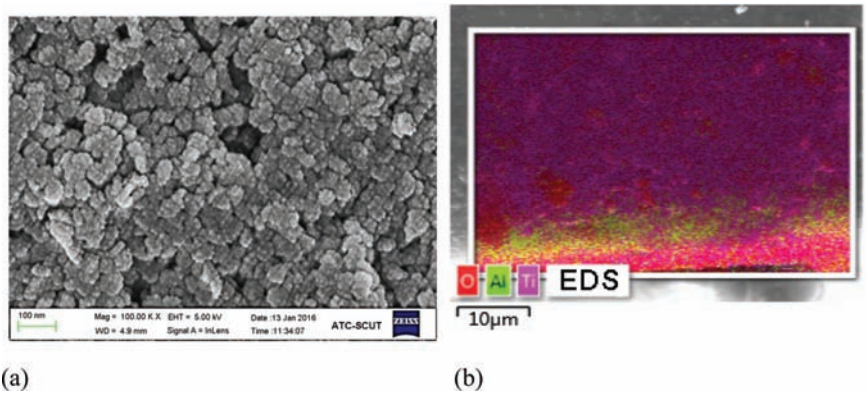

Figure 15. SEM and EDS images on the surface of honeycomb aluminium mesh of the photo-catalytic reactor. (a) SEM image in the direction perpendicular to the gas flow; (b) EDS elemental mapping in the direction parallel to the gas flow: oxygen (red), aluminium (green), titanium (purple).

4.3.1 Blank experiments and optimal experiments

4.3.1.1 Blank experiments

Before the photo-catalytic degradation study, some blank experiments of the experimental system and the optimal experiments of the photo-catalytic reactor were conducted as the descriptions in Section 3.3.2.

Firstly, according to the operations in Table 2, five blank experiments were conducted and the results were plotted in Figure 16. Giving the following:

(1) In the No.1 blank experiment, without the honeycomb aluminium mashes in the chamber, the formaldehyde was slightly degraded under the illumination of UV lamps, and the degradation rate was 20% in 120 minutes.
(2) In the No.2 blank experiment, without the honeycomb aluminium meshes and formaldehyde in the chamber, the indication of the formaldehyde sensor increased over the time, which implied that the formaldehyde sensor was sensitive to the ozone produced by the UV lamps.
(3) However, in the No.3 blank experiment, when the honeycomb aluminium meshes added, the formaldehyde sensor did not detect anything, which indicates

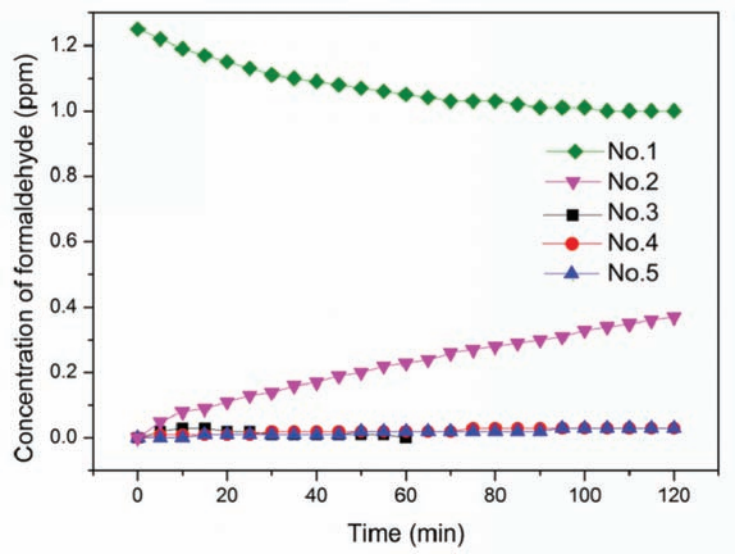

Figure 16. Five blank experiments of the experimental system. No.1: UV(√) Net(×) HCHO(√); No.2: UV(√) Net(×) HCHO(×); No.3: UV(√) Net(√) HCHO(×); No.4: UV(×) Net(√) HCHO(×); No.5: UV(×) Net(×) HCHO(×).

that the ozone produced by the UV lamps was degraded by the titanium dioxide coated nanoparticles on the honeycomb aluminium meshes [33].

(4) Results of the No.4 and No.5 blank experiments indicate no presence of formaldehyde in the experiments, which implies that the honeycomb aluminium meshes and the chamber themselves do not induce any pollutions into the photo-catalytic oxidation system.

4.3.1.2 Optimal experiments

After having confirmed that the experimental chamber honeycomb aluminium meshes do not provide any substances, a series of process optimization experiments were conducted to investigate the optimal conditions of the photo-catalytic reactor. Three elements influencing the photo-catalytic degradation were considered in the study: (A) Gas flowrate; (B) Number of the photo-catalytic components; (C) Geometry of the honeycomb aluminium mesh.

(A) Gas flowrate

Varying the fan speed in the range [32.4, 324] $m^3\ h^{-1}$, the influence of gas flowrate on the photo-catalytic degradation of formaldehyde was shown in Figure 17. Two groups of data could be observed, higher flowrates (324 and 259.2 $m^3\ h^{-1}$) and lower flowrates (162, 97.2 and 32.4 $m^3\ h^{-1}$). At higher flowrates, the photo-catalytic degradation process was slower and took longer time to be completely degraded due to the shorter residence time of formaldehyde in the photo-catalytic reactor.

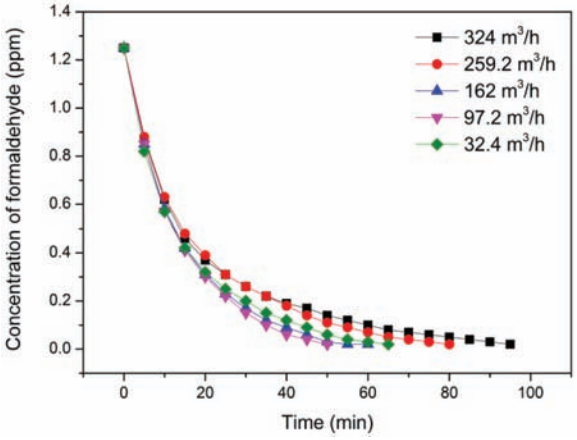

Figure 17. Influence of gas flowrate on the photo-catalytic degradation process.

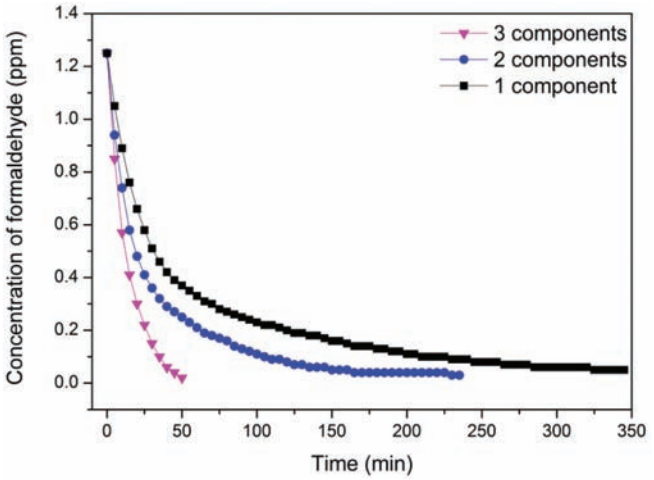

Figure 18. Influence of the number of photo-catalytic components on the photo-catalytic degradation process.

(B) Number of the photo-catalytic components

Varying the equipped number of photo-catalytic components in the reactor from one to three (Figure 18), the time for the same amount of formaldehyde to be degraded completely decreased from 345, 235 to 50 minutes, respectively. From Figure 18 it is obvious that the photo-catalytic components play an important role in the oxidation behaviour of the reactor. Being illuminated under UV lamps, the formaldehyde passes through the components, adsorb on the nanoparticles coated on the honeycomb aluminium meshes and is degraded. More photo-catalytic components give more surface area and thus increases the photo-catalytic degradation rate.

(C) Size of the honeycomb aluminium mesh

Since the mesh size of the honeycomb aluminium mesh would influence the resistance for gas to pass, two mesh sizes (2 mm and 3 mm) were compared in the study, see Figure 19. The photo-catalytic degradation performance with 2 mm mesh was slightly better to that with 3 mm mesh, it took 45 and 50 minutes for the same amount of formaldehyde being completely degraded with 2 mm mesh and 3 mm mesh, individually. The smaller the mesh size, the higher the gas resistance, and the longer residence time on the photo-catalytic components.

According to the above experiments, the optimal operational parameters of the reactor were identified as follows: a gas flowrate of 97.2 $m^3 h^{-1}$ (Figure 17), three

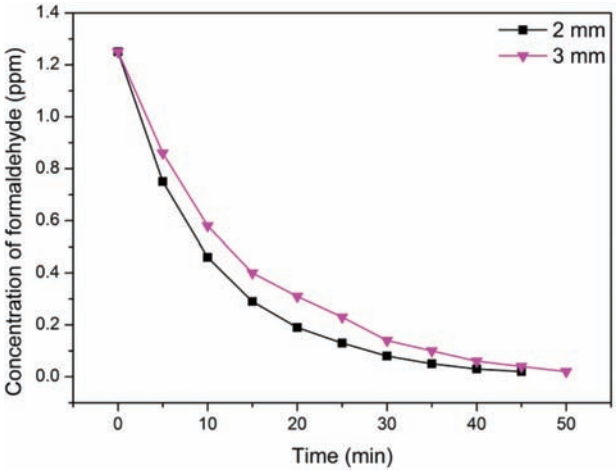

Figure 19. Effect of the honeycomb aluminium mesh size on the photo-catalytic degradation process.

photo-catalytic components (Figure 18) and 2 mm size of the honeycomb aluminium mesh (Figure 19).

4.3.2 Photo-catalytic oxidation of gaseous pollutants detected in paper mills

After the blank experiments and the optimizations experiments, photo-catalytic oxidation of the gaseous pollutants detected in the paper mills were tested with the optimal conditions. Given to the results in Sections 4.1 and 4.2, three kinds of substances were applied to assess the degrading performance of the developed photo-catalytic reactor: (A) Formaldehyde; (B) Benzene; (C) Mixture of formaldehyde and benzene.

4.3.2.1 Formaldehyde as the target pollutant

The experimental results of degrading formaldehyde with different initial concentrations are given in Figure 20. These show that the developed photo-catalytic reactor could completely degrade the formaldehyde independent of the initial concentration. As indicated in Figure 19, the times needed for complete degradation were 41 minutes, 35 minutes and 30 minutes for 2.5 ppm, 1.5 ppm and 0.5 ppm initial concentrations of formaldehyde, respectively.

Although the degradation profile varies at initial concentrations of formaldehyde (Figure 20(a)), after normalization with respect to these initial concentrations,

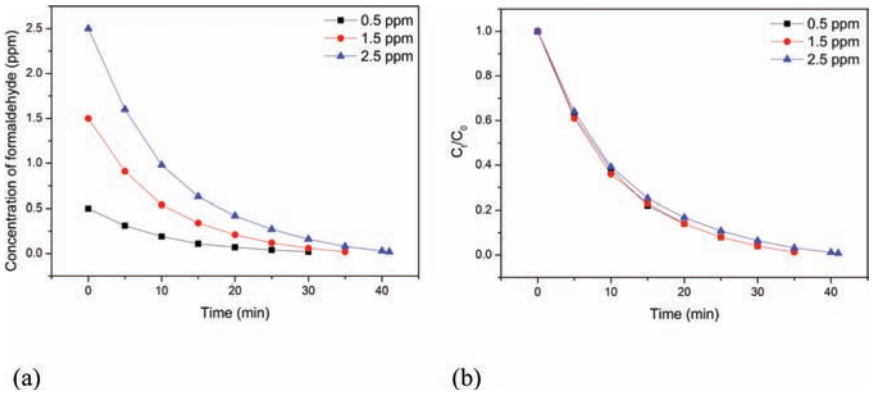

Figure 20. Influence of initial formaldehyde concentration on the degradation under optimal conditions. (a) Degradation of formaldehyde, (b) Degradation of formaldehyde with the normalized concentration.

Figure 20(b), the curves coalesce to the same curve. Thus, the degradation process is given as:

$$C(t) = C_0 e^{-0.1t} \tag{4}$$

where, t is the degradation time, $C(t)$ is the formaldehyde concentration at time t, C_0 is the initial concentration of formaldehyde.

4.3.2.2 Benzene as the target pollutant

Under the optimal conditions, the experimental results for the degradation of benzene with different initial concentrations are shown in Figure 21. Compared to Figure 20, and as revealed in Figure 21, although the photo-catalytic reactor could completely degrade benzene in 310 minutes, 180 minutes, and 70 minutes for 2.5 ppm, 1.5 ppm and 0.5 ppm initial concentrations of benzene, respectively, the degradation processes were considerably longer than those for formaldehyde degradation at the same initial concentration. And the degradation behaviour in Figure 21(a) is very different from that of formaldehyde. When the initial concentration of benzene increases, the time for being totally degraded in principle increases linearly. Furthermore, normalization of benzene concentration with initial conditions (Figure 21(b)), gives a different result compared to formaldehyde. The degradation rate depends significantly on the initial benzene concentration. This observation is in agreement with what was observed by Ma *et al.* [34].

In Figure 22, the degradation profiles of formaldehyde and benzene at the same initial concentration of 1.25 ppm is plotted. From the graph, it is evident that it takes almost four times longer to degrade benzene than formaldehyde, the reason for this could be:

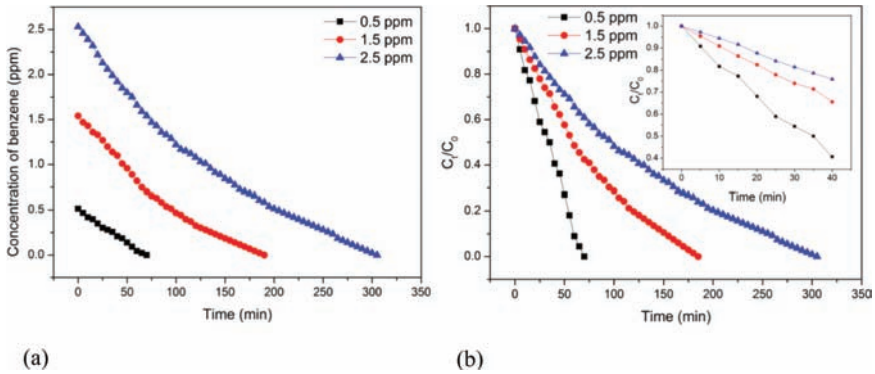

Figure 21. Influence of initial benzene concentration on the degradation under the optimal conditions. (a) Degradation evolution of benzene, (b) Degradation evolution of benzene with the normalized benzene concentration.

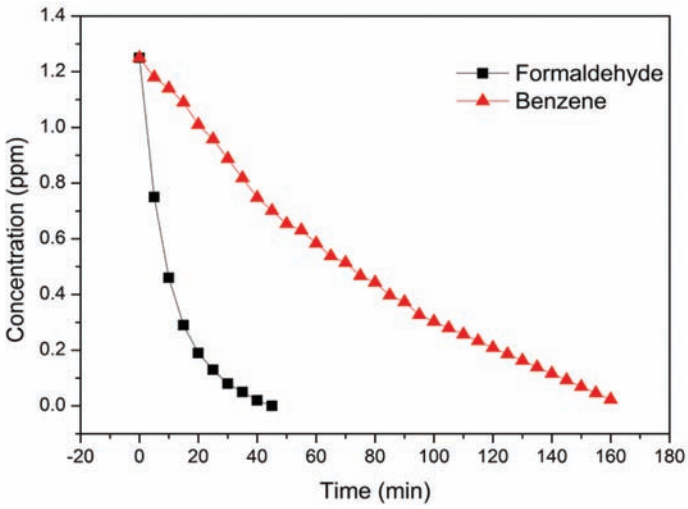

Figure 22. Comparison of the degradation profiles of formaldehyde and benzene with the same initial concentration.

(1) Formaldehyde has only one carbon atom, and formic acid has been identified as the main intermediate during its photo-catalytic degradation. The pathway for the photo-catalytic degradation of formaldehyde is short and it could be completely converted into CO_2 and H_2O at the end of the degradation process [35].
(2) In comparison, the pathway for the photo-catalytic degradation of benzene is long and complex [36], it includes several internal processes: direct hole oxidation, hydroxyl radical reaction and polymerization.
(3) Moreover, benzene homologues are not easily adsorbed by the catalyst at room temperature. Although intermediates can be strongly adsorbed on the surface of catalyst, they are less reactive. Therefore, the competitive adsorptions of the intermediate products and the catalyst deactivation might be the main factors causing the slow degradation process of benzene [36, 37].

4.3.2.3 Mixture of formaldehyde and benzene as the target pollutant

Since there is a mixture of gaseous pollutants in paper mills, a mixture of formaldehyde and benzene was applied to further assess the degradation performance of the reactor. Having set the initial concentrations of formaldehyde and benzene at about 0.625 ppm each, giving a total initial concentration of 1.25 ppm. The effect on photo-catalytic degradation can be found in Figure 23.

Firstly, as for the degradation behaviour of formaldehyde in Figure 23, as for the case of pure formaldehyde, the concentration of formaldehyde decreased rapidly in the initial phase; but the degradation rate gradually slows down, and even becomes slower than that of benzene at the end of the process. Also, the formaldehyde could not be completely degraded. Secondly, with respect to the degradation behaviour of benzene, the concentration of benzene decreased relatively slowly in the initial stage, then fast decreased to be completely degraded at a relatively constant rate.

For the purpose of comparison, the degrading processes of formaldehyde and benzene in their pure forms (Figures 20(a) and 21(a)) and the mixed form (Figure 23) were replotted in Figure 24.

It can be seen in Figure 24(a) that, with the same initial concentrations of formaldehyde, the reaction process in the mixture was different from that in its pure form, and it took more than 3 times as long to be degraded, and it is clearly seen that is not completely degraded. In comparison in Figure 24(b), not only the time behaviour of the degradation of benzene is almost the same for the mixture and pure form, but also the degradation processes in the mixed form was faster than that in its pure form. The phenomena in Figure 23 could be discussed as follows:

(1) In the initial reaction phase, since benzene was not easily adsorbed on the catalyst, the formaldehyde in the mixture was mainly adsorbed on the catalyst and degraded.

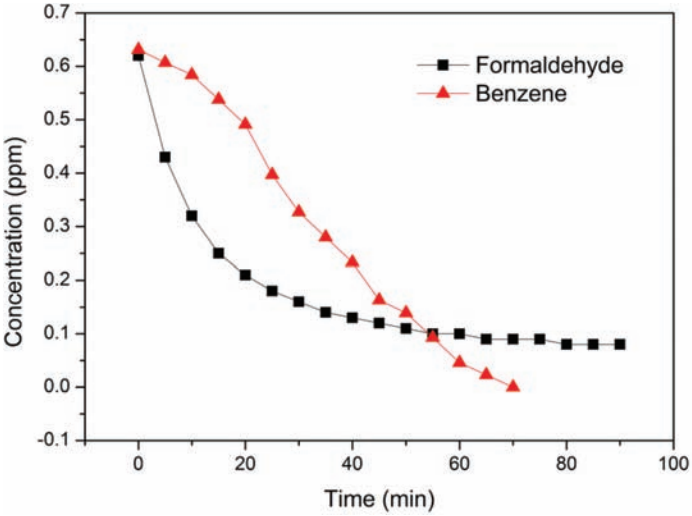

Figure 23. Degradation evolution of the mixture of formaldehyde and benzene under the optimal conditions.

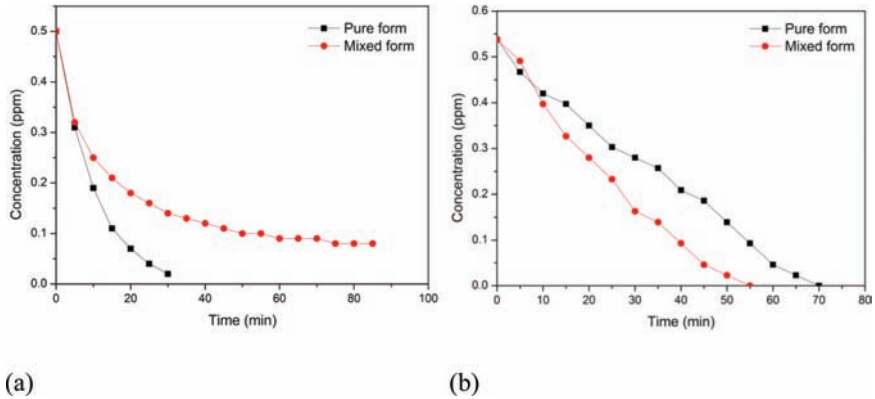

Figure 24. Comparisons of the degradation profiles of (a) formaldehyde and (b) benzene in their pure and mixed forms

(2) With the photo-catalytic degradation of formaldehyde, the adsorption and degradation of benzene in the mixture became dominant gradually.
(3) The competitive adsorptions of intermediate products generated from the photo-catalytic degradation of benzene slowed down the degradation of formaldehyde in the mixture.

(4) Due to the influences of aldehyde substances generated in the degradation process of benzene [36, 38], our used formaldehyde sensor maybe also sensitive to the aldehyde group, thus its indications might not represent the real concentrations of formaldehyde.

Summarizing Section 4.3, a photo-catalytic reactor was developed and its performance with respect to degradation of formaldehyde and benzene were studied. After having conducted the blank experiments and the optimization experiments, the performance tests of the reactor showed that:

(1) Formaldehyde could be completely degraded.
(2) Benzene could also be completely degraded but more slowly.
(3) The behaviour of a mixture of formaldehyde and benzene was more complex, where benzene could still be totally degraded, but a non-zero concentration of formaldehyde was observed finally.

CONCLUSIONS

The studies on the gaseous pollutions in pulp and paper mills have been scarce for a long time. Aiming at this situation, this paper investigated the gaseous pollutions in five pulp and paper mills quantitatively, each mill having different production processes, raw materials and final products; following this, the detailed compositions of VOCs in one mill were determined using GC-MS. Finally, the performance of a developed photo-catalytic reactor was evaluated using formaldehyde and benzene.

The results were concluded as follows:

- Part 1: Analysis results of ambient air samples in five pulp and paper mills.
  - The levels of TVOC, HCHO, H_2S, and C_xH_y in pulp mills were much higher than those in paper mills.
  - Different raw materials and applied paper chemicals could largely influence the gaseous pollutions in paper mills.
  - The most serious gaseous pollutants on the wet-end of paper machine and the wastewater treatment plant were both TVOC and H_2S.
- Part 2: GC-MS determination results of VOCs in the ambient air samples of one mill.
  - The benzene homologues were the main components of VOCs.
  - The phenols were detected on all the sampling sites.
- Part 3: Photo-catalytic oxidation of gaseous pollutants.
  - According to the analysis results of gaseous pollutants in pulp and paper mills, three kinds of pollutants were selected to assess the degrading

performance of the developed photo-catalytic reactor: (1) Formaldehyde; (2) Benzene; (3) Mixture of formaldehyde and benzene.

- The photo-catalytic reactor basically had excellent degradation performances under the optimal conditions.

ACKNOWLEDGMENTS

The research was supported by the Research Funds of National Science Foundation of Guangdong, China (No. 2016A030313478), Science and Technology Planning Project of Guangdong, China (No. 2015A020215012), State Key Laboratory of Pulp and Paper Engineering (Nos. 2017ZD03 and 2015C05), and Science and Technology Program of Guangzhou, China (No. 201607010050).

REFERENCES

1. R. Chandra and M. Sankhwar. Influence of lignin, pentachlorophenol and heavy metal on antibiotic resistance of pathogenic bacteria isolated from pulp paper mill effluent contaminated river water. *J. Environ. Biol.* **32**(6): 739–745, 2011.
2. M. Kamali and Z. Khodaparast. Review on recent developments on pulp and paper mill wastewater treatment. *Ecotox. Environ. Safe.* **114**: 326–342, 2015.
3. Z. G. Wen, J. H. Di and X. Y. Zhang. Uncertainty analysis of primary water pollutant control in china's pulp and paper industry. *J. Environ. Manage.* **169**: 67–77, 2016.
4. T. Meyer and E. A. Edwards. Anaerobic digestion of pulp and paper mill wastewater and sludge. *Water Res.* **65**: 321–349, 2014.
5. J. S. Kiurski, B. B. Maric, S. M. Aksentijevic, I. B. Oros, V. S. Kecic and I. M. Kovacevic. Indoor air quality investigation from screen printing industry. *Renew. Sust. Energ. Rev.* **28**: 224–231, 2013.
6. A. Lattuati-Derieux, S. Bonnassies-Termes and B. Lavédrine. Characterisation of compounds emitted during natural and artificial ageing of a book. Use of headspace-solid-phase microextraction/gas chromatography/mass spectrometry. *J. Cult. Herit.* **7**(2): 123–133, 2006.
7. Y. Tao, C. Y. Wu, and D. W. Mazyck. Removal of methanol from pulp and paper mills using combined activated carbon adsorption and photocatalytic regeneration. *Chemosphere.* **65**(1): 35–42, 2006.
8. H. H. Suh, T. Bahadori, J. Vallarino and J. D. Spengler. Criteria air pollutants and toxic air pollutants. *Environ. Health Persp.* **108**: 625–633, 2000.
9. X. Zhen, H. Li, W. Zhang and T. Ma. Performance research and optimization on toluene condensation recovery system. *Cryogenics Superconductivity* **43**(2): 67–73, 2015.
10. J. Huang, W. Zhao, L. Chen, Z. Wang, Y. Shi and F. Zhang. The applications of absorption process for VOCs gases of benzene. *Guangdong Chemical Industry* **38**(223): 79–80, 2011.

11. W. He, G. Xie, H. Wu, H. Sha and Y. Xu. The overview about harm of VOCs waste gas and treatment technology. *Sichuan Chemical* **01**: 16–18, 2012.
12. L. Zhao, Y. Zhang, R. Li and Z. Ma. The harm of VOC and recycling and processing technology. *Chemical Education* **16**: 1–6, 2015.
13. H. Wang, Y. Liu, D. Peng, F. Wang and M. Lu. The development of membrane separation technology and its application prospect. *Applied Chemical Industry* **42**(3): 532–534, 2013.
14. D. Ravelli, D. Dondi, M. Fagnoni and A. Albini. Photocatalysis. A multi-faceted concept for green chemistry. *Chem. Soc. Rev.* **38**(7): 1999–2011, 2009.
15. S. Wang, H. M. Ang and M.O. Tade. Volatile organic compounds in indoor environment and photocatalytic oxidation: state of the art. *Environ. Int.* **33**(5): 694–705, 2007.
16. T. C. An, L. Sun, G. Y. Li, Y. P. Gao and G. G. Ying. Photocatalytic degradation and detoxification of o-chloroaniline in the gas phase: mechanistic consideration and mutagenicity assessment of its decomposed gaseous intermediate mixture. *Appl. Catal. B: Environ.* **102**(1): 140–146, 2011.
17. L. Sun, G. Y. Li, S. G. Wan and T. C. An. Mechanistic study and mutagenicity assessment of intermediates in photocatalytic degradation of gaseous toluene. *Chemosphere* **78**(3): 313–318, 2010.
18. J. Y. Chen, G. Y. Li, Z. G. He and T.C. An. Adsorption and degradation of model volatile organic compounds by a combined titania-montmorillonite-silica photocatalyst. *J. Hazard. Mater.* **190**(1): 416–423, 2011.
19. X. Fan, T. L. Zhu, Y. F. Sun and X. Yan. The roles of various plasma species in the plasma and plasma-catalytic removal of low-concentration formaldehyde in air. *J. Hazard. Mater.* **196**: 380–385, 2011.
20. W. Liang, J. Li and Y. Jin. Photo-catalytic degradation of gaseous formaldehyde by TiO_2/UV, Ag/TiO_2/UV and Ce/TiO_2/UV. *Build. Environ.* **51**: 345–350, 2012.
21. GB 50325-2010. Code for indoor environmental pollution control of civil building engineering, 2010.
22. X. Tong, Z. Liu, X. Q. Chen and W. H. Shen. Analysis and pollution sources speculations of toxic gases in a secondary fiber paper mill. *J. Environ. Sci. Heal A* **51**: 1149–1156, 2016.
23. GB/T18883-2002. Quality standards for indoor air, 2002.
24. GB 14554-93. Emission standards for odor pollutants, 1994.
25. National Institute for Occupational Safety and Health (NIOSH). Methane-International Chemical Safety Cards, 1994. http://www.cdc.gov/niosh/ipcsneng/neng0291.html (accessed 16.10.07).
26. National Institute for Occupational Safety and Health (NIOSH). Occupational Exposure to Alkanes (C5-C8), 1977. http://www.cdc.gov/niosh/docs/1970/77-151.html (accessed 16.10.07).
27. M. Sainlez and G. Heyen. Comparison of supervised learning techniques for atmospheric pollutant monitoring in a Kraft pulp mill. *J. Comput. Appl. Math.* **246**: 329–334, 2013.
28. E. M. Ekstrand, M. Larsson, X. B. Truong, L. Cardell, Y. Borgstrom, A. Bjorn, J. Ejlertsson, B. H. Svensson, F. Nilsson and A. Karlsson. Methane potentials of the

Swedish pulp and paper industry – A screening of wastewater effluents. *Appl. Energ.* **112**: 507–517, 2013.

29. V.Sricharoenchaikul. Assessment of black liquor gasification in supercritical water. *Bioresource Technol.* **100**: 638–643, 2009.
30. G.-L. Zhang, Y. Liang, J.-Y. Zhu, Q. Jia, W.-Q. Gan, L.-M. Sun and H.-M. Hou. Oxidative stress-mediated antiproliferative effects of furan-containing sulfur flavors in human leukemia Jurkat cells. *Food Chem.* **180**: 1–8, 2015.
31. R. Kubec, P. Krejcova, L. Mansur and N. Garcia. Flavor precursors and sensory-active sulfur compounds in alliaceae species native to South Africa and South America. *J. Agr. Food Chem.* **61**:1335–1342, 2013.
32. X. Tong, Z. Zhang, X. Chen and W. Shen. Analysis of volatile organic compounds in the ambient air of a paper mill: A case study. *BioResources* **10**: 8487–8497, 2015.
33. Y. Lu, X. Zhao, M. Wang, Z. Yang, X. Zhang and C. Yang. Feasibility analysis on photocatalytic removal of gaseous ozone in aircraft cabins. *Build. Environ.* **81**: 42–50, 2014.
34. J. Ma, C. Zhu, J. Lu, H. Liu, L. Huang, T. Chen and D. Chen. Catalytic degradation of gaseous benzene by using TiO_2/goethite immobilized on palygorskite: Preparation, characterization and mechanism. *Solid State Sci.* **49**: 1–9, 2015.
35. W. Liang, J. Li and Y. Jin. Photo-catalytic degradation of gaseous formaldehyde by TiO_2/UV, Ag/TiO_2/UV and Ce/TiO_2/UV. *Build. Environ.* **51**: 345–350, 2012.
36. O. D'Hennezel, P. Pichat and D. F. Ollis. Benzene and toluene gas-phase photocatalytic degradation over H_2O and HCL pretreated TiO_2: by-products and mechanisms. *J. Photoch. Photobio. A* **118**(3): 197–204, 1998.
37. Q. Zhang, F. Zhan and G. Zhang. Reaction mechanism of gas-phase photocatalytic oxidation of benzene on TiO_2. *Chinese J. Catal.* **25**(1): 39–43, 2004.
38. X. Wang, G. Zhang, F. Zhang and Y. Wang. Progress in photocatalytic degradation of volatile aromatics in gas phase over titanium dioxide. *Chem. Res. Appl.* **18**(4): 344–353, 2006.

Transcription of Discussion

QUANTITATIVE STUDIES OF AMBIENT GASES IN PULP AND PAPER MILLS AND THEIR DEGRADATION WITH PHOTO-CATALYTIC OXIDATION TECHNOLOGY

Xin Tong, Wenhao Shen and Xiaoquan Chen

State Key Laboratory of Pulp and Paper Engineering, South China University of Technology, Guangzhou, 510640, P.R. China

Wolfgang Bauer Graz University of Technology

Where do you plan to use the developed reactor? And what is the maximum throughput that you can send through this reactor. Looking at the degradation curves the reactions appear quite slow taking up to 40 minutes. The volume of gases that you have in paper or pulp mill is quite high, so the capacity of your reactor after upscaling would be of interest?

Xin Tong South China University of Technology

The concentrations we used for the formaldehyde in the degradation is much higher than the concentrations in the real paper mills, so I think in the real situations, it will work better.

Jean-Claude Roux Grenoble Institute of Technology

I would like to know how the gas pollutant goes in the photoreactor. Can you give us some details? I mean, by leaching, or by going through the filter paper? My question is, how does it work?

Discussion

Xin Tong

We can see in the slide, the titanium dioxide was covered on a honeycomb aluminum net. We can see the SEM pictures on the corner. The titanium dioxide covering the net produced the degradation under the UV light.

Jean-Claude Roux

I was wondering if titanium dioxide was on or in the filter. You answered, it is on the honeycomb network. Thank you very much.

Peter De Clerck PaperTec Solutions Pte Ltd

What is the source of the benzene that you are finding throughout the mill process?

Xin Tong

I think there are many kinds of chemical additives found in the process, but they are the homologous compounds, so we use the simple ones as the object compounds and we choose the benzene.

Peter De Clerck

So, this was a model compound, not something that you are actually finding in the mill environment? There are very strict controls on benzene and chemicals for use in paper outside of China. I was very surprised to see benzene there as a detected pollutant in the air systems.